Available online at www.sciencedirect.com
SCIENCE DIRECT®
Journal of Power Sources 128 (2004) 292–307
JOURNAL OF POWER SOURCES
www.elsevier.com/locate/jpowsour

Design and simulation of a lithium-ion battery with a phase change material thermal management system for an electric scooter

Siddique A. Khateeb [a], Mohammed M. Farid [b], J. Robert Selman [a], Said Al-Hallaj [a,*]

[a] *Center for Electrochemical Science and Engineering, Department of Chemical and Environmental Engineering, Illinois Institute of Technology, Chicago, IL 60616, USA*

[b] *Department of Chemical and Materials Engineering, University of Auckland, Auckland, New Zealand*

Received 21 August 2003; accepted 27 September 2003

Abstract

A lithium-ion battery employing a novel phase change material (PCM) thermal management system was designed for an electric scooter. Passive thermal management systems using PCM can control the temperature excursions and maintain temperature uniformity in Li-ion batteries without the use of active cooling components such as a fan, a blower or a pump found in air/liquid-cooling systems. Hence, the advantages of a compact, lightweight, and energy efficient system can be achieved with this novel form of thermal management system. Simulation results are shown for a Li-ion battery sub-module consisting of nine 18650 Li-ion cells surrounded by PCM with a melting point between 41 and 44 °C. The use of aluminum foam within the PCM and fins attached to the battery module were studied to overcome the low thermal conductivity of the PCM and the low natural convection heat transfer coefficient. The comparative results of the PCM performance in the presence of Al-foam and Al-fins are shown. The battery module is also simulated for summer and winter conditions. The effect of air-cooling on the Li-ion battery was also studied. These simulation results demonstrate the successful use of the PCM as a potential candidate for thermal management solution in electric scooter applications and therefore for other electric vehicle applications.

Keywords: Lithium-ion battery; Thermal management; Phase change materials; Electric scooter; Thermal modeling/simulation; Air-cooling

1. Introduction

The automotive market demands high specific power and high specific energy density batteries to meet the operational needs of electric vehicles without adding substantial weight to the vehicle. Lead–acid batteries have served the battery market needs for more than a century in terms of cranking power, life and low cost [1]. Lead–acid batteries face a tough challenge to meet these criteria while advanced battery technology such as nickel-metal hydride (NiMH) and lithium-ion batteries have demonstrated superior performance compared to lead–acid batteries. Table 1 summarizes the characteristics of few commercially available rechargeable batteries. As shown in Table 1, lithium-ion batteries have four to five times higher energy density than the lead–acid batteries, which makes them suitable for electric vehicles providing longer range, sufficient acceleration and high calendar life [2]. Although, NiMH batteries is currently the battery of choice in hybrid electric vehicle (HEV), Li-ion battery has twice the energy density of NiMH battery and if the thermal safety issue is successfully addressed, Li-ion batteries have the potential to replace the NiMH battery for HEV applications.

In order to achieve the power demand in electronics or propulsion power in an electric vehicle, a number of Li-ion cells have to be connected in series and parallel to form a battery pack. Hence, the safety of the battery pack and electric vehicle apart from the user becomes a big concern owing to their higher volumetric heat generation rate as compared to valve-regulated lead–acid (VRLA) or NiMH battery [3]. Hence, effective heat dissipation and thermal runaway safety are the major concerns in the commercialization of Li-ion batteries for high power applications. Therefore, a successful thermal management solution is required. There exists a strong interdependence between the temperature distribution within the battery and electrochemical performance [4], which would require a proper thermal management system for optimal performance of these battery packs. Consequently, temperature uniformity and heat dissipation are important factors in the development of thermal management systems for Li-ion batteries. An ideal thermal management system should be able to maintain the battery pack at an optimum temperature with small variations within

* Corresponding author. Tel.: +1-312-567-5118; fax: +1-312-567-6914.
E-mail address: alhallaj@iit.edu (S. Al-Hallaj).

0378-7753/$ – see front matter © 2003 Elsevier B.V. All rights reserved.
doi:10.1016/j.jpowsour.2003.09.070

Nomenclature

m_{PCM} mass of the PCM (kg)
C_p specific heat of the PCM (J/(g K))
C_{p_e} effective specific heat of the PCM ((J/(g K))
T_m PCM melting point (K)
T_i PCM initial temperature (K)
λ latent heat of the PCM (kJ/kg)
Q_{disch} Li-ion battery discharge heat (kJ)

the modules and within the pack and also meet the other requirements namely compact, light-weight, easy packaging, inexpensive, low parasitic power demand features. [3].

Conventional heat dissipation methods such as forced air-cooling and liquid-cooling have been extensively developed as thermal management tools for electric vehicles. Such thermal management systems may prove to be effective but they tend to make the overall system too bulky, complex and expensive in terms of blower, fans, pumps, pipes and other accessories, which add on to the system weight and parasitic power requirements [3].

A novel thermal management solution, which uses phase change material (PCM) as a heat dissipation source, was proposed for electric and hybrid electric vehicle applications [6]. The major advantages for such a thermal management system are a compact, inexpensive, low maintenance system with no parasitic power requirements. A Li-ion battery system for electric vehicle applications such as electric bikes, electric two to four wheeled scooter, electric cars and hybrid electric vehicles requires a well-designed thermal management system with a reliable safety circuit design. In this paper, a Li-ion battery design with a PCM thermal management system is presented and simulated for a Zappy electric scooter model no. 02815B (ZAP, Santa Rose, CA). Results show that a PCM thermal management system appears to be an ideal thermal management solution for electric scooters given the vehicle space constraints and absence of auxiliary power sources.

Table 2
Specifications of Zappy electric scooter model no. 02815 (*source*: Zappy Technical Manual [7])

Features	Specifications
Operating voltage	12 V dc
Battery	Sealed, maintenance free lead–acid battery
Battery dimension	7 in. × 7 in. × 3 in.
Battery weight	12.5 lbs (5.7 kg)
Speed	11–13 mph (17.7–20.9 km/h)
Driving range	8 miles[a]
Motor	Permanent magnet direct current motor
Motor power	0.5 hp at 3500 rpm peak
Motor control	Single speed, solid state/electro-mechanical system
Drive train	Silent belt drive
Brakes	Rear band brake, hand operated
Overall dimension	Length: 41 in.; width: 11 in.; height: 11 in.
Overall weight	37 lbs (16.8 kg)

[a] On level ground, depends on the rider's weight and road inclination.

The Zappy electric scooter is a lightweight, foldable electric scooter powered by a 12 V, 18 Ah lead–acid battery. The specifications of the Zappy electric scooter are summarized in Table 2.

Fig. 1(a) shows the Zappy electric scooter in the folded view and Fig. 1(b) shows its full view. The electric motor is located at the rear end and the battery is situated at the bottom as shown in the figure.

2. Development of Li-ion battery for the Zappy electric scooter

The detailed outline in developing the Li-ion battery may be summarized as follows.

2.1. Performance evaluation of the electric scooter

This test was conducted to verify the manufacturer's specifications for the electric scooter. Various parameters such as the mileage, speed, battery charge/discharge time were

Table 1
Characteristics of the rechargeable batteries [5]

	NiMH	Lead–acid	Li-ion	Li-ion polymer
Gravimetric energy density (Wh/kg)	60–120	30–50	110–160	100–130
Internal resistance (includes peripheral circuits) (mW)	200–300, 6 V pack	<100, 12 V pack	150–250, 7.2 V pack	200–300, 7.2 V pack
Cycle life (to 80% of initial capacity)	300–500	200–300	500–1000	300–500
Fast charge time	2–4 h	8–16 h	2–4 h	2–4 h
Overcharge tolerance	Low	High	Very low	Low
Self-discharge/month (room temperature)	30%	5%	10%	~10%
Cell voltage (nominal)	1.25 V	2 V	3.6 V	3.6 V
Load current				
Peak	5 C	5 C	>2 C	>2 C
Best result	0.5 C or lower	0.2 C	1 C or lower	1 C or lower
Operating temperature (discharge only)	−20 to 60 °C	−20 to 60 °C	−20 to 60 °C	0–60 °C
Maintenance requirement	60–90 days	3–6 months	Not required	Not required
Commercial use since	1990	1970	1991	1999

Fig. 1. (a) and (b) Zappy electric scooter model no. 02815B (*source*: Zappy Technical Manual [5]).

determined under different operating conditions such as variation in the load, level and inclined road conditions.

From these tests, it was concluded that the Zappy electric scooter did not meet the performance specifications set by the manufacturer; however, these results have to be verified with few more scooters. The average speed was around 8 mph (13 km/h) with a medium and heavy weight rider on a level ground; the driving range was about 5 miles (8 km) for a fully charged battery. These tests were performed with varying loads and different road conditions. The average charging time of the lead–acid battery was around 8 h. From this test, the performance limits of the electric scooter were set and will be used for comparison with the Li-ion battery.

2.2. Electrical characterization test

This test is carried out in order to determine the size of the battery needed to meet the power requirements. The voltage–current characteristics of the battery and the electric motor characteristics were obtained by using an onboard data acquisition system (DAQ). Various time-series data were recorded by the DAQ system such as the current, voltage and the motor temperature.

Fig. 2 shows the results obtained from the test run of the Zappy scooter on a relatively flat ground with small inclines with rider weighing 145 lbs (65 kgs).

The following conclusions were drawn based on the preliminary vehicle test results:

- the surge current during the start-up of the electric motor was around 50–55 A;
- the average current during the scooter operation on a flat ground was found to be 18–24 A, which is the current rating of the present lead–acid battery in the Zappy electric scooter;
- the current requirements of the battery during an uphill can easily reach 60 A;
- the temperature of the lead–acid battery remains between 20 and 30 °C;
- the temperature of the electric motor rises to 70 °C from a start temperature of 20 °C.

Since the temperature rise of the lead–acid battery is not significant as compared to NiMH and Li-ion battery, the lead–acid battery does not require a thermal management system in this electric scooter. In lead–acid battery, the discharge reaction of the battery is not highly exothermic

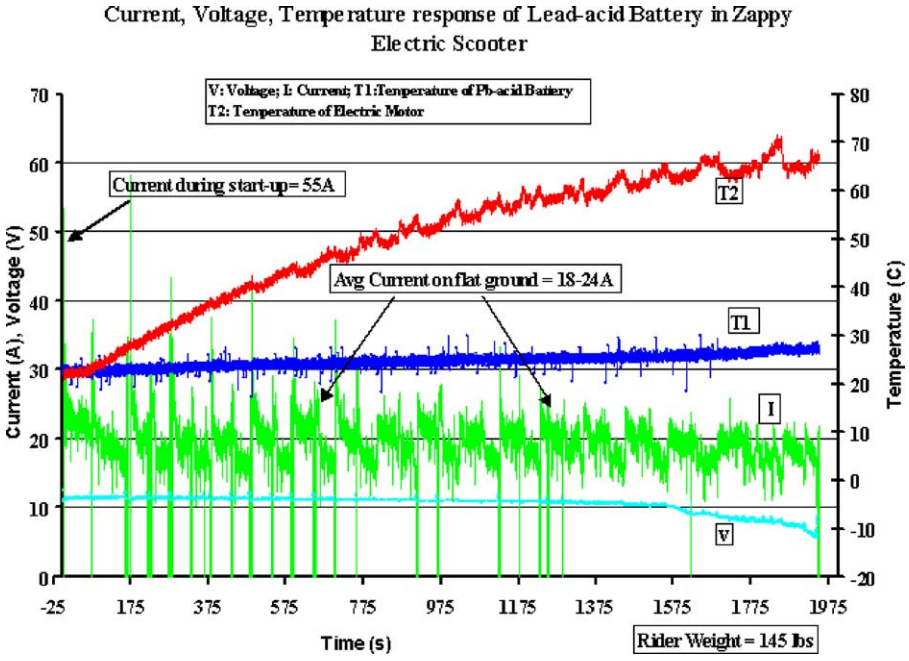

Fig. 2. Preliminary testing of Zappy electric scooter.

Table 3
Specifications of the 18650 Li-ion cell

Nominal voltage	3.67 V
Nominal capacity	2.0 Ah
Energy	7.34 Wh
Size	Diameter: 18 mm; length: 65 mm
Weight	42 g
Energy density	
Gravimetric	160 Wh/kg
Volumetric	300 Wh/l
Charge duration	2–4 h (100%) 1 h (80%)
Operating specifications	
Operating voltage	4.2–3.0 V
Charge voltage	4.2 V ± 50 mV
Cut-off voltage	3.0 V
Temperature range	−20 to 60 °C

as compared to NiMH and Li-ion battery and hence, do not require a sophisticated, well-designed thermal management system. In general, most of the commercially available light-weight electric scooters employing lead–acid battery do not contain a cooling system.

With the above current requirements, it is now possible to design a Li-ion battery module configuration. The 18650 type Li-ion cells were used in designing the Li-ion battery to power the Zappy electric scooter.

The specifications of a commercial 18650 type Li-ion cell are summarized in Table 3.

2.3. Li-ion battery prototype design

The Li-ion battery prototype for the Zappy electric scooter is designed in order to replace the existing lead–acid battery given the space and operational constraints.

The Li-ion battery for the Zappy electric scooter will consist of two modules each containing 18 cells. Each module consists of six strings with three cells in series while the six strings of cells are connected in parallel. The nominal voltage and capacity of each module is 11.1 V and 12 Ah, respectively.

The current and voltage requirement of the Zappy electric scooter is 20–24 A and 10–12 V, respectively under the normal operating conditions on a flat ground. Hence, two modules have to be connected in parallel to meet the current requirements. During the start-up of the vehicle, the current requirement is 55 A for 300 ms and each string of the module would discharge at 2.4 C rate for 300 ms. Here, the C-rate refers to the amount of current supplied/withdrawn for a specific time period during the charge/discharge of the Li-ion cell [5]. The Li-ion battery module design is shown in Fig. 3.

2.4. Onboard Li-ion battery module safety circuit

The Li-ion cell should be protected against any danger of overcharge, which can cause undesirable effects on the battery operation and thermal protection [8].

All the six strings in the module will be connected with a safety circuit which is rated at 5 A and 12 V. This can ensure safe monitoring of each string of Li-ion cells for overcharge and short-circuit danger. The safety circuits from the two modules will be integrated together to meet the total current requirement.

2.5. Thermal characterization of the Li-ion cells

The heat generation of the Li-ion cell used in the simulation is based on the experimental data obtained from accelerating rate calorimeter (ARC). ARC experiments are carried out to determine the amount of heat generated by the cell during the charge and discharge cycle. Selman et al. [9] reported the heat generation values of four different commercial 18650 Li-ion cells using ARC-Arbin battery cycler set-up. The ARC-battery cycler experimental set-up is described elsewhere [10,11]. The heat generation results of the 1.5 Ah Panasonic 18650 Li-ion cells were chosen and scaled up to 2 Ah Li-ion cells, which is the capacity of the commercially available cells today.

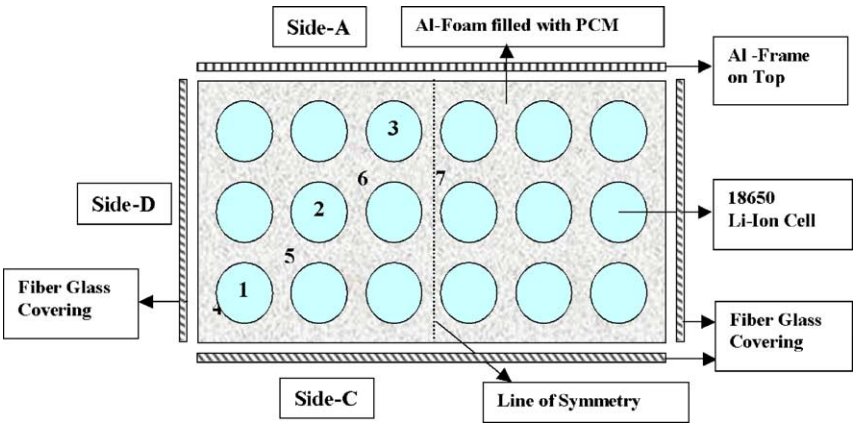

Fig. 3. Li-ion battery in the Zappy scooter.

2.6. Simulation of the Li-ion battery module

The Li-ion battery module consists of 18 cells arranged in three rows with six cells in each row as shown in Fig. 3. Two battery modules are placed adjacent to each other in the Zappy electric scooter in such a way that each module rests on one of its longer sides, side C. When the scooter is moving, the side edges of the battery are exposed to forced air circulation. The battery compartment is made up of fiberglass on three sides and covered on top by the aluminum scooter frame. Side A is assumed to be in close contact with this frame and the bottom side C and other sides B and D are also assumed to be in close contact with the fiberglass.

A single sub-module containing nine cells was simulated because of the symmetry in arrangement of the cells and similar boundary conditions of the battery. Forced cooling was assumed to take place on three sides (A, C and D) of the battery during the discharge of the battery module when the scooter is moving and adiabatic condition along the other side (line of symmetry). The heat transfer coefficient during forced cooling was calculated to be 20 W/(m^2 K) using a heat transfer correlation available in literature [12]. During the battery charge, when the scooter has stopped only free convection cooling is assumed to take place on the three sides of the module (A, C and D). The heat transfer coefficient during free or natural convection was considered to be 5 W/(m^2 K) [12]. The simulations are carried out for continuous three cycles representing the most abusive battery operation.

It is assumed that the battery box surfaces are in close contact with the battery compartment sides in the present Zappy scooter design. The existing battery design and its orientation in the battery compartment can replace the existing lead–acid battery in the Zappy scooter without making any design changes. Modifications to the battery compartment have to be made in an alternative design to incorporate the aluminum fins on the battery compartment.

The initial temperature of the Li-ion battery module was assumed to be 30 °C in the simulations, except during the summer and winter conditions where the initial temperature was 40 and 0 °C, respectively.

2.7. Modeling and simulation of the Li-ion battery module with air-cooling thermal management system

A simplified unsteady-state two-dimensional thermal model [2] was employed for simulating the Li-ion cell operation. The simulations were conducted for three discharge/charge cycles to verify the thermal stability of the battery module.

The sub-module shown in Fig. 3 is simulated to understand the thermal effect of the module during the battery operation with air-cooling. The air flowing in between the Li-ion cells is assumed to be in natural convection with a heat transfer coefficient of 5 W/(m^2 K) [12], since the box is covered completely on all sides. Also, the space available for the battery in the scooter is constrained which makes it difficult to accommodate any kind of air-flow passage, ducting, fans that may be required for forced air-cooling of the module.

In the Zappy electric scooter, there exists an aluminum frame casing, which covers the electric motor and the battery box, as shown in Fig. 1. There is a close contact between the battery box and the aluminum frame, which can dissipate the heat during the battery discharge. This aluminum frame increases the heat transfer area available for heat dissipation. In order to show the benefit of this large heat transfer area on heat dissipation rate, the sub-module is simulated with aluminum fins attached on the external sides of the battery space provided in the Zappy scooter.

The temperature profiles of the Li-ion cell and the surrounding air are shown in Fig. 4. The temperature of the Li-ion cell at center location (3) rises by 45 °C whereas the cell exposed to forced air-cooling during discharge at location (1) (in Fig. 3) rises by 35 °C, with a temperature gradient of 10 °C between the cells. There also exists a large temperature gradient of about 20 °C between the air at the center of the module and the air exposed to forced air-draft convection at the outer location. Such thermal gradients within a battery module can result in unequal charge/discharge capacity of the individual cells over the cycle life. Wright et al. [20], conducted several experiments with Li-ion cells exposed to various temperatures and showed that the cell capacity degrades significantly affecting the calendar life when exposed to a temperature >60 °C. Also, the onset of the thermal runaway reaction of the Li-ion cells starts in the temperature range of 70–100 °C depending on the electrolyte composition and electrode material [13]. As a result, the Li-ion cell in this case is prone to a thermal runaway risking the safety of the battery and vehicle.

In order to reduce the temperature rise of the Li-ion cells, the heat transfer coefficient of the surrounding air has to be increased significantly, which can be achieved only via forced air-cooling which adds to complexity in design incorporating fans if needed, ducting and other accessories. All these features require major modifications in the existing scooter. But even with forced air-cooling, external power is required to keep the cooling system operational which raises a question of safety risk in case of external power breakdown or mechanical failure of any of its components.

2.7.1. The need for a passive thermal management system

An especially difficult problem that must be addressed by an active cooling system is the battery temperature rise when the vehicle is parked on a hot day. Nelson et al. [14] analyzed the consequences of a battery temperature rise of up to 45 °C in the absence of active cooling when the vehicle is turned off. Under such circumstances, starting the car again can result in the battery temperature exceeding safe limits. They showed that a dedicated refrigeration system is necessary to keep the battery at close to ambient temperatures during the warm summer months. Increasing the amount of insulation

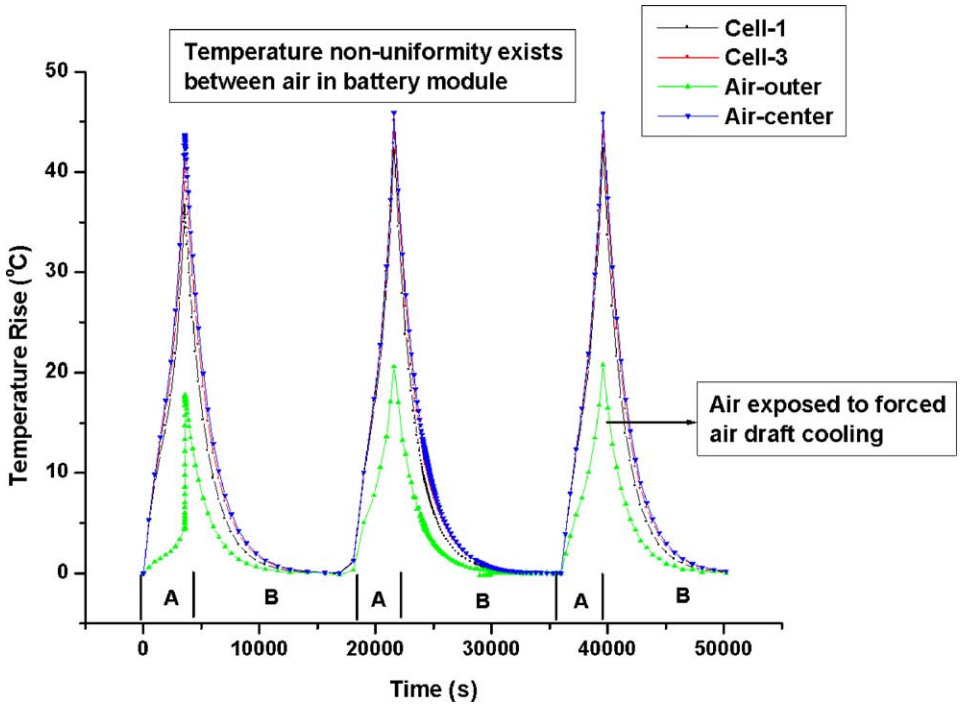

Fig. 4. Temperature rise of the Li-ion cells and air ($h = 5\,W/(m^2\,K)$).

around the battery was considered, but this increases design complexity and adds further parasitic power requirements when the vehicle is turned off.

On the other hand, this problem can be solved relatively simply without any additional power requirement by a passive thermal management system via phase change material integrated cooling system (with proper PCM mass and temperature optimization). It is not suggested that active cooling is completely unnecessary when using PCM integrated cooling. But the design and control of the active component is much simplified. However, to achieve this simplicity, PCM integration has to be considered from the outset. In our opinion, retrofitting will not work.

Recently, EV Global Motors Co., which manufactures electric scooters with Li-ion batteries recalled 2000 Li-ion batteries in Mini E-bike electric bicycles, after it received five reports of battery over-heating, three of which caught fire [15]. The main reason for this incident was the absence of a thermal management system for the Li-ion batteries. The Li-ion battery in this case depended on the natural air-cooling of the battery alone for heat dissipation, which proved to be disastrous because of insufficient cooling.

Nelson et al. [14] discuss the disadvantages of an air-cooling system in detail for Li-ion batteries for hybrid electric vehicle applications. They concluded that air-cooling system requires high power because of the large volume of air required at low speed, as well as large cross-sections in the flow passages from and to the supply and exit manifolds. Also, parallel air-flow channels must be provided to all modules, which further complicates design and wastes battery power. Liquid-cooling, which has not

Table 4
Properties of paraffin wax [6]

Melting temperature	40–44 °C
Latent heat	195 KJ/kg
Specific heat capacity	1.77 KJ/kg K
Thermal conductivity	
Solid phase	0.21 W/m K
Liquid phase	0.29 W/m K
Density	
Solid phase	822 kg/m^3
Liquid phase	910 kg/m^3

Table 5
Specifications of the Li-ion battery module with PCM system for Zappy electric scooter

Specifications	Value
No. of modules	2
No. of 18650 Li-ion cells per module	18
Weight of the cells	756 g
Volume of the cells	297 cm^3
Weight of the PCM	216 g
Volume of the PCM	237 cm^3
Weight of Al-foam, safety circuits, battery box (approximately)	250 g
PCM/battery weight ratio	28.6%
PCM/battery volume ratio	79.7%
Dimensions of the battery box	Length: 15 cm; width: 7.8 cm; height: 7.5 cm
Total weight of the Li-ion battery/module	1.2 kg (2.7 lbs)

yet been introduced anywhere, may allow smaller cooling flow cross-sections, but barely yield a reduction in mass flow rates and cooling channel mass.

Toyota Prius employs a sophisticated air-cooling thermal management for the NiMH batteries (whose heat generation is much less than that of Li-ion batteries) [16]. The control strategy employed in the Toyota Prius forces the NiMH battery to utilize only part of its power capability and about 40% of the total charge of the battery, thus sacrificing the battery capacity and power for longer cycle life and to control

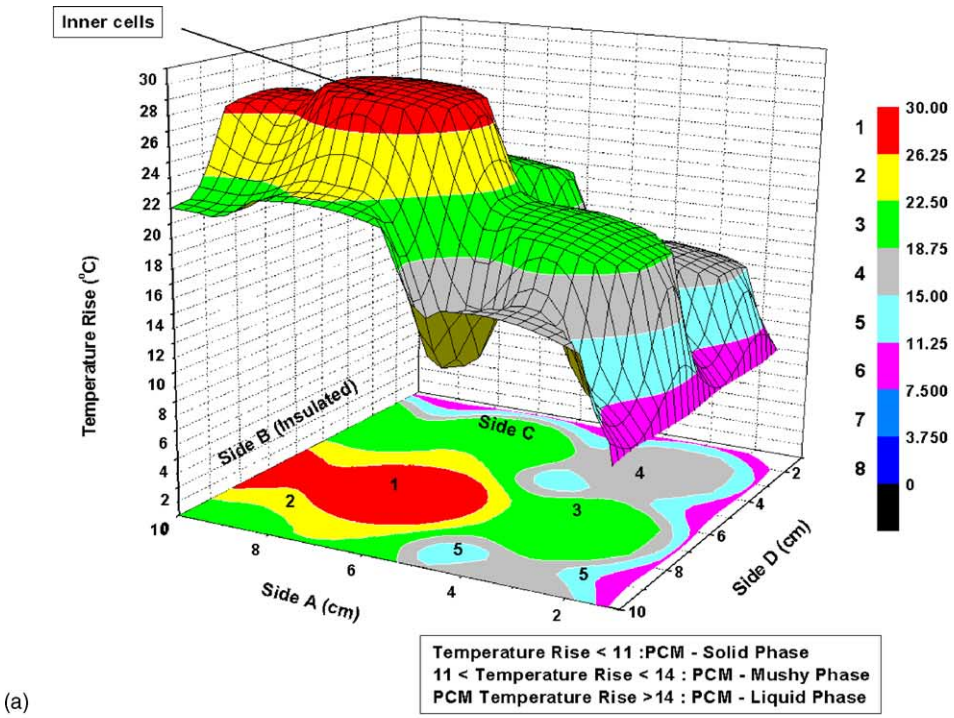

(a)

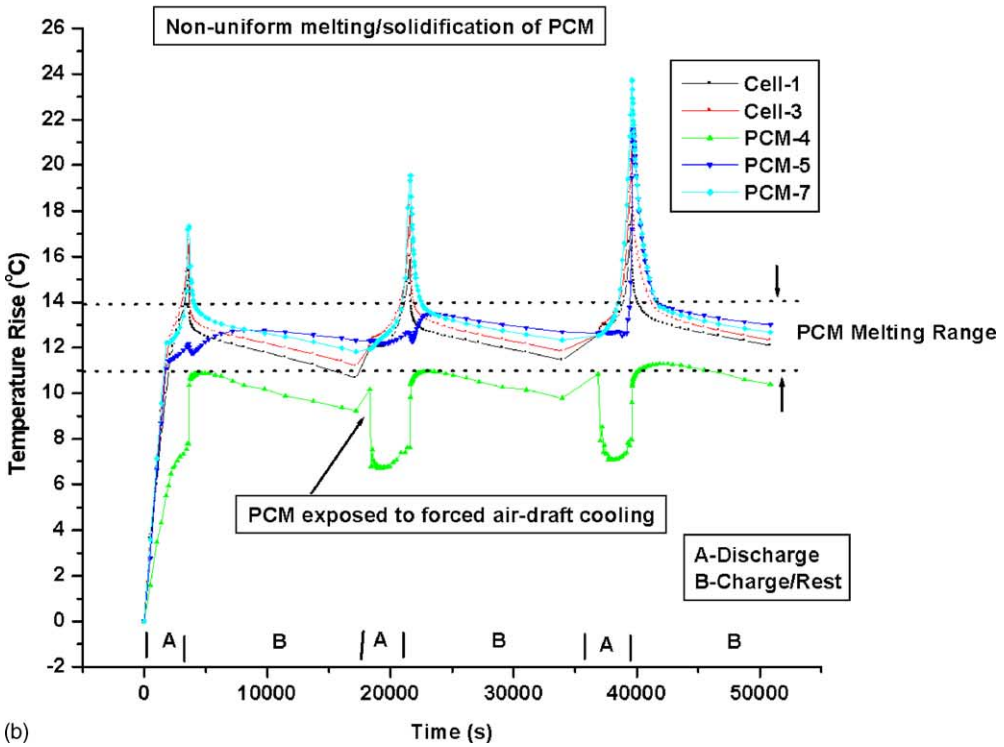

(b)

Fig. 5. (a) Temperature contours of Li-ion cells and PCM. (b) Temperature rise of Li-ion cells and PCM. (c) Effective specific heat of PCM.

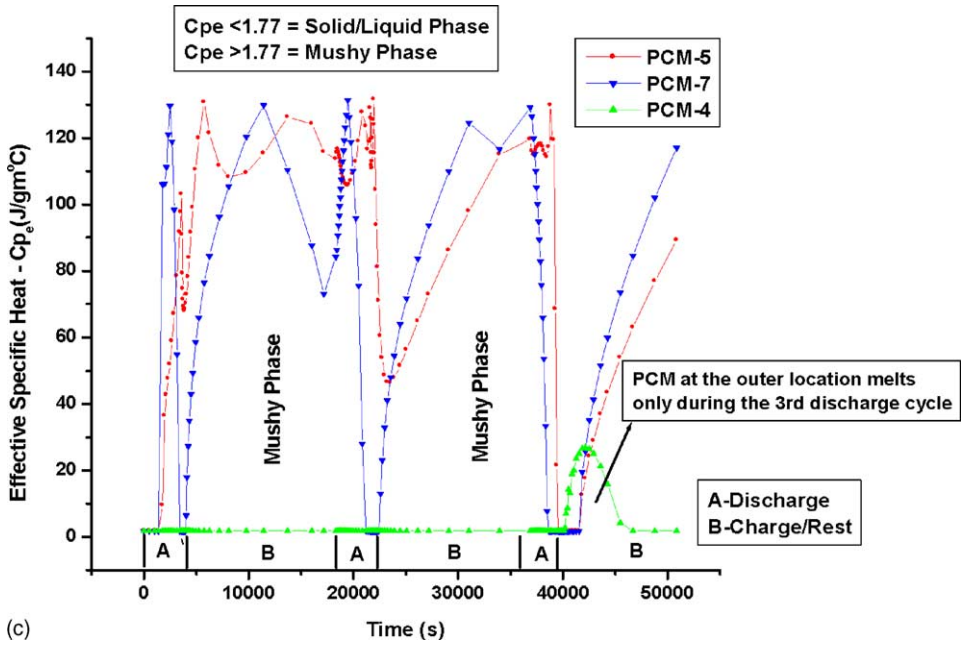

Fig. 5. (*Continued*).

the temperature rise due to specific thermal and mechanical design constraints of the air-cooling system.

Implementing a PCM thermal management system can avoid the above-mentioned disadvantages of the air-cooling system, limited battery capacity and power use with a well-designed optimized PCM system. The thermal response of the Li-ion battery in the presence of a PCM will be explored in the next few sections.

2.8. Phase change material (PCM) thermal management system design

Based on the heat generation data from the ARC results [9], the mass of the PCM required is calculated as follows:

heat discharged by the battery

= sensible heat of the PCM + latent heat of the PCM

$$Q_{\text{disch}} = m^*_{\text{PCM}} C^*_p (T_{\text{m}} - T_{\text{i}}) + m^*_{\text{PCM}} \lambda \quad (1)$$

The properties of the Paraffin wax used as a PCM for Li-ion batteries thermal management are as shown in Table 4.

The quantity of the PCM required was calculated to be approximately 12 g for each 18650 Li-ion cell. Hence, for a Li-ion battery module consisting of 18 cells, the total mass of the PCM is 216 g. The specifications of the Li-ion battery prototype are summarized in Table 5.

Another issue to be addressed with the PCM system is the volume expansion encountered upon solidification of the PCM after melting, which can induce mechanical stress on the battery pack casing. This was accounted for in the battery design by allowing an additional 10% volume in the battery pack casing. Also, the battery casing has to be completely leak-proof to avoid any possible leaks of the PCM when it is in the liquid phase.

3. Modeling and simulation results for the phase change material thermal management system

A simplified unsteady-state two-dimensional thermal model [2] was employed for simulating the Li-ion cell operation. The PCM was modeled using an effective heat capacity method as explained elsewhere [17]. The simulations were conducted for three discharge/charge cycles to verify the thermal stability of the battery module. The temperature rise of the Li-ion cells and PCM shown in simulation are at the numbered locations shown in Fig. 3.

3.1. Analysis of the effective specific heat curves in simulation

The effective specific heat (C_{p_e}) accounts for the latent heat, in the phase change region which gives an indication of the extent of melting and solidification of the PCM. The values of C_{p_e} change from a small value of the solid phase to a maximum value of the order of a hundred or less at the melting temperature [17]. Rising peaks in the effective specific heat curves of the PCM show the transition from the solid phase to the mushy phase during the discharge of the battery. Higher values of the effective specific heat ($1.77 < C_{p_e} < 130$) denote the latent heat of melting/solidification of the PCM; the higher the peaks, the greater the extent of melting. Smaller peaks in the curves signify little melting of

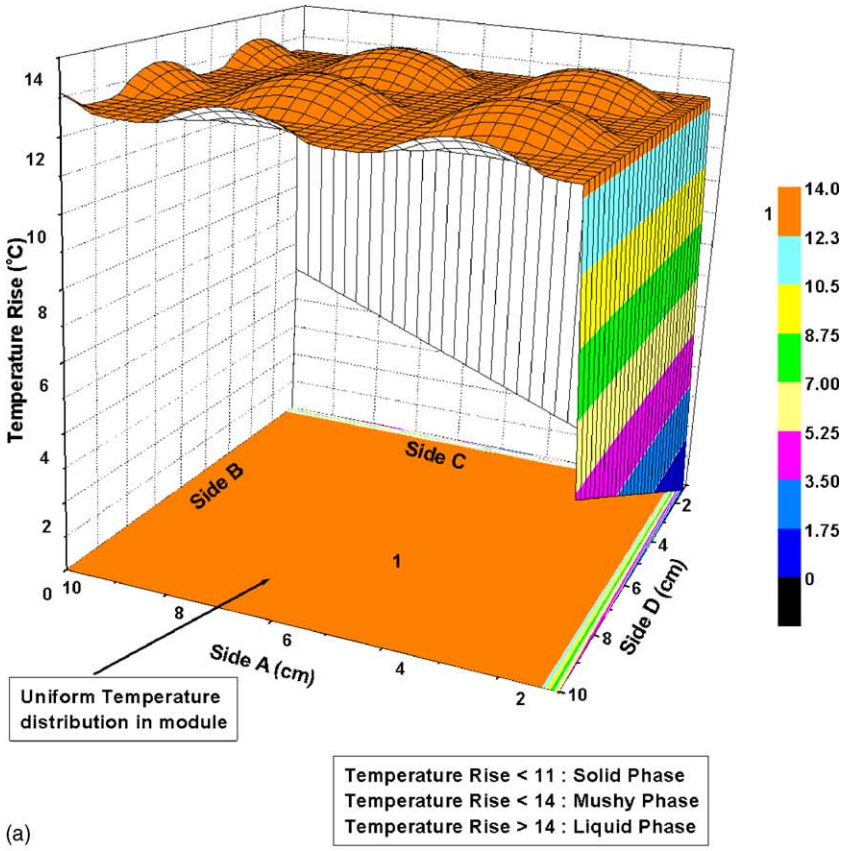

(a)

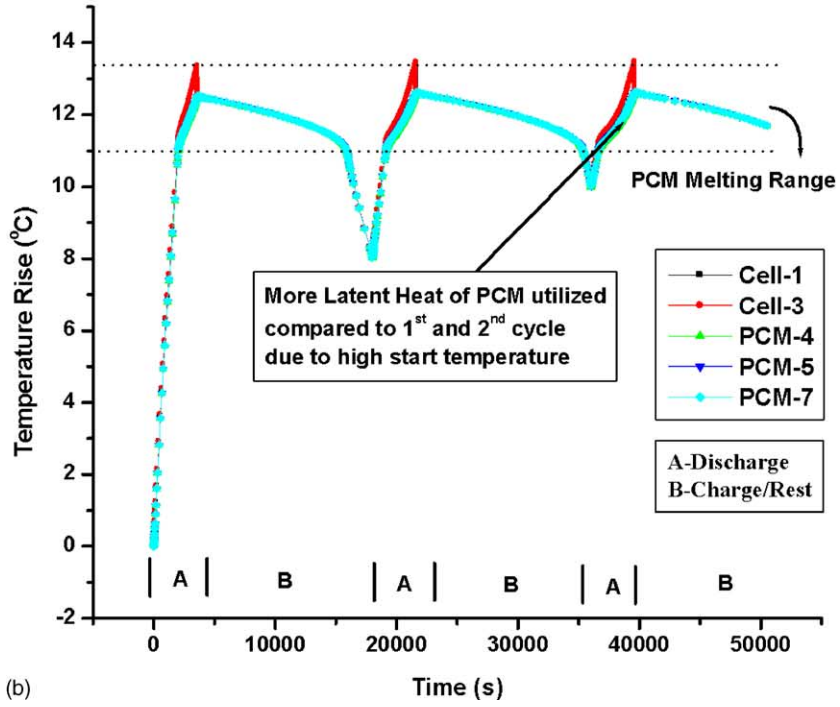

(b)

Fig. 6. (a).Temperature contours of Li-ion cells and PCM in Al-foam. (b) Temperature rise of Li-ion cells and PCM in Al-foam. (c) Effective specific heat of PCM in Al-foam.

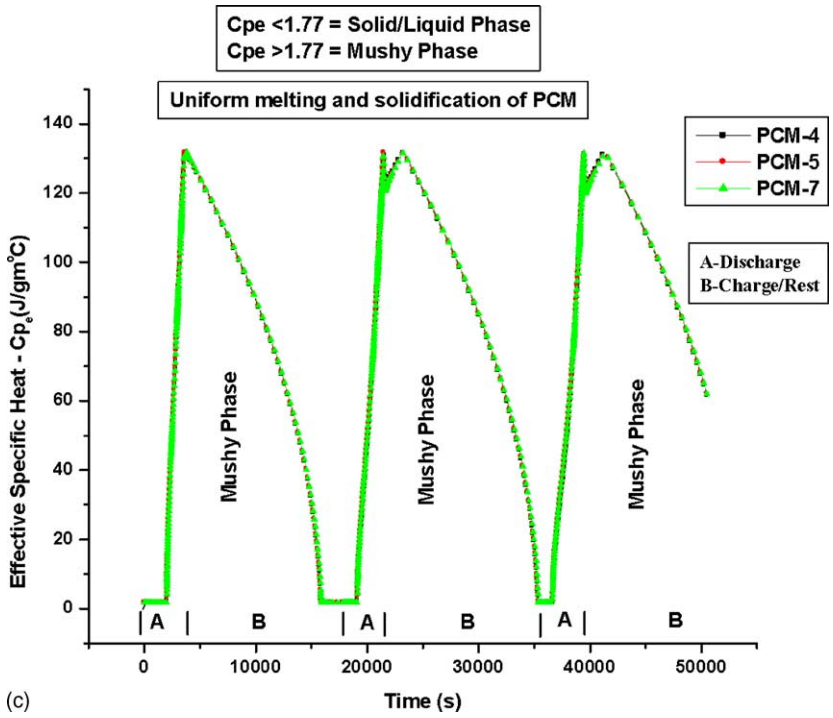

Fig. 6. (*Continued*).

the PCM. When the PCM has completely melted, the peaks drop down showing the transition from the mushy phase to the liquid phase. During the rest period when the temperature of the Li-ion cells and the PCM drops, the PCM changes into the mushy phase again, represented by a broad peak. The width of the peaks during the melting and solidification stages signifies the time length of the PCM transition from solid-mushy phase (melting-battery discharge period) and liquid-mushy phase (solidification-battery rest/charge period), respectively. Usually, the width of the peaks is narrow during the PCM melting when the battery is discharging and broad during solidification of PCM under the battery rest/charge condition.

3.2. Case study 1

3.2.1. Li-ion battery module with PCM alone

Fig. 5(a) shows the temperature contours of the module at the end of the third discharge cycle. In Fig. 5(a), one side is modeled as perfectly insulated (due to line of symmetry) and the other three sides (A, C and D) are subjected to forced cooling when the scooter is moving. As seen from the module arrangement, the cell at the center of the module experiences the highest temperature rise compared to the other cells as indicated in Fig. 5(a). The non-uniformity in temperature distribution of the Li-ion cells and the PCM in the module is clearly represented by the different contours shown in Fig. 5(a).

The temperature distribution of the cells and the PCM during the three cycles is shown in Fig. 5(b). The scooter is assumed to stop after 1 h of use for the battery to be charged. The normal charging period for the Li-ion batteries is usually 2–4 h [9]. During this period, cooling of the battery is assumed to occur by natural convection cooling. In the first cycle of discharge, complete melting takes place at the center location (7) with only partial melting at location (5) and very little melting at location (4) exposed to forced air-draft cooling during discharge; these locations are shown in Fig. 3. During the following charge period, the post-discharge heat evolution from the cells causes the temperature of the PCM increases slightly whereas the temperature of the cells keeps decreasing. But due to poor thermal conductivity of the PCM, the PCM at locations (5) and (7) remain in the mushy phase at the end of the first cycle whereas the PCM at location (4) solidifies due to little melting experienced during discharge.

During the second and the third discharge cycles, the PCM at the inner locations are in the mushy phase at the beginning, which causes the temperature of the cells and the PCM to increase significantly. The latent heat of the PCM is completely utilized during the pre-discharge period resulting in complete melting of PCM at inner locations turning them into liquid phase. The temperature of the cells starts rising along with the liquid PCM. Fig. 5(c) shows the effective specific heat profiles of the different PCM locations. The PCM at locations (5) and (7) show peaks during the three cycles indicating their melting and solidification during discharge and charge cycles. The PCM at the outer end of the module exposed to forced air-convection during discharge starts melting during the third discharge cycle

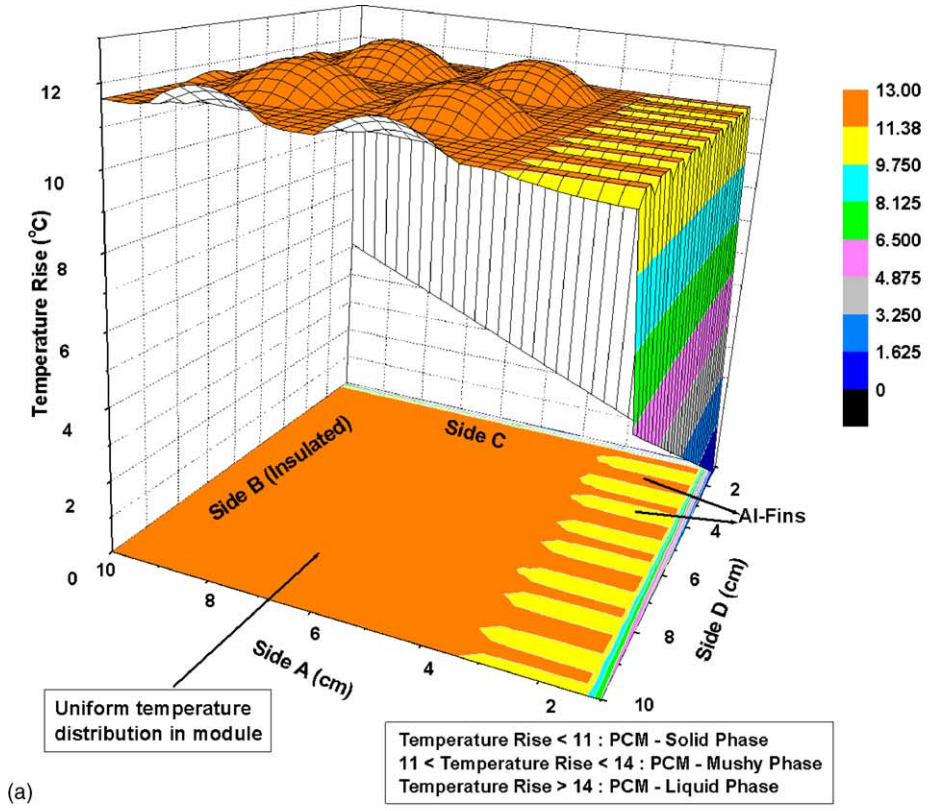

(a)

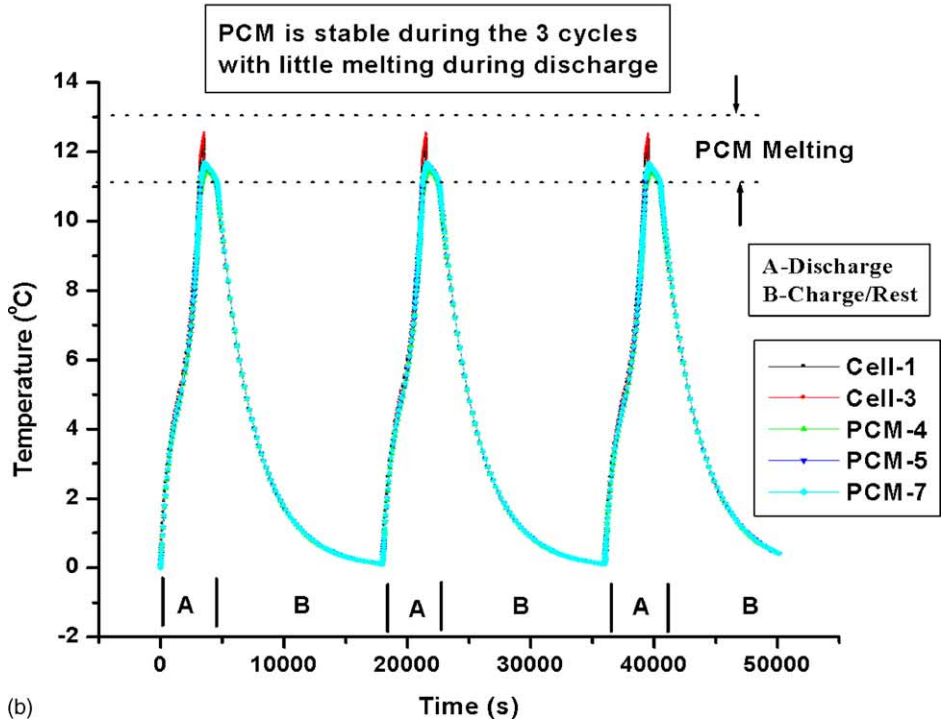

(b)

Fig. 7. (a) Temperature contours of Li-ion cells and PCM in Al-foam with Al-fins. (b) Temperature rise of Li-ion cells and PCM in Al-foam with Al-fins. (c) Effective specific heat of PCM in Al-foam with Al-fins.

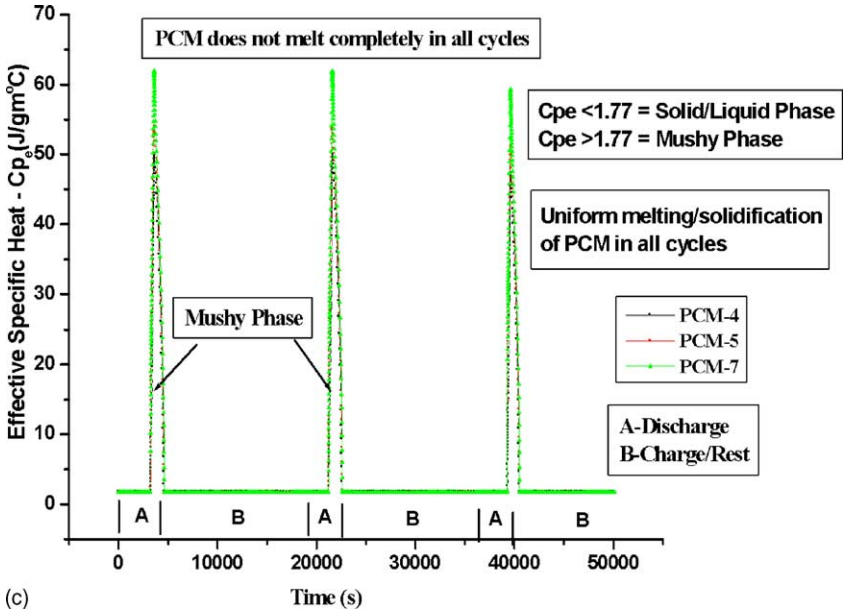

Fig. 7. (*Continued*).

indicated by the small peak with no peaks during the previous cycles.

Hence, the effect of the poor thermal conductivity of the PCM is evident, resulting in non-uniform temperature distribution in the module and ineffective heat dissipation. The performance of the Li-ion cell is strongly dependent on the temperature, which affects its cyclic capability and capacity retention. Li-ion cells exposed to higher temperature can result in higher capacity fade and faster aging [16], resulting in an imbalance in terms of charge acceptance and discharge capability of the cells in the module. As a measure of improving the thermal performance of the phase change material, the effect of the encapsulating the PCM in aluminum-foam in studied in the next section.

3.3. Case study 2

3.3.1. PCM with Al-foam

In this simulation, the poor thermal conductivity of the PCM is overcome by using aluminum foam. Commercially available Duocel aluminum foam with a density of 8–10% and 40 ppi (pores per inch) was used for this purpose [18]. The aluminum foam used enhances the thermal conductivity of the PCM approximately by one order of magnitude or greater. The effective thermal conductivity, which accounts for the combined conduction through the aluminum foam material and the PCM, which fills up the voids, was calculated to be approximately 3 $W/(m^2 K)$ [19].

Fig. 6(a) and (b) clearly show the uniform temperature distribution throughout the entire PCM and the cells as compared to Fig. 5(a) and (b), due to the encapsulation of the PCM in the Al-foam. Fig. 6(a) shows the temperature contours of the module. There are no multiple temperature interface boundaries between cell–PCM and PCM–PCM similar to that shown in the previous case for PCM alone (i.e. Fig. 5(a)). The role of the aluminum foam in fast heat dissipation can be observed in Fig. 6(b). After the first discharge cycle of the battery, the PCM is completely melted in the module similar to the previous case but solidification of the PCM occurs during the charge/rest period. In the second discharge cycle, the temperature of the module begins at 8 °C higher than the first cycle. Although the temperature rise is almost same as the first discharge cycle, more latent heat of the PCM is utilized. In the third discharge cycle, the initial temperature of the module is close to the melting point of the PCM. The temperature rise is relatively same compared to the previous cycles because the latent heat of the PCM is utilized more at the beginning of discharge period.

The effective specific heat curves in Fig. 6(c) indicate the uniform melting and solidification of the PCM during the three cycles. Although, the addition of aluminum foam created a uniform temperature distribution in the module and a stable thermal response of the PCM as compared to the previous case, it is desired to operate each discharge cycle from the same initial temperature operating condition. The next simulation study demonstrates the effect of adding aluminum fins to achieve this goal.

3.4. Case study 3

3.4.1. PCM with Al-foam and Al-fins

This conceptual design incorporating aluminum fins is suggested as an alternative design of the existing Zappy scooter design. In the previous case study, the thermal response of the Li-ion cells and the PCM was not stable in the consecutive cycles, resulting in a different starting

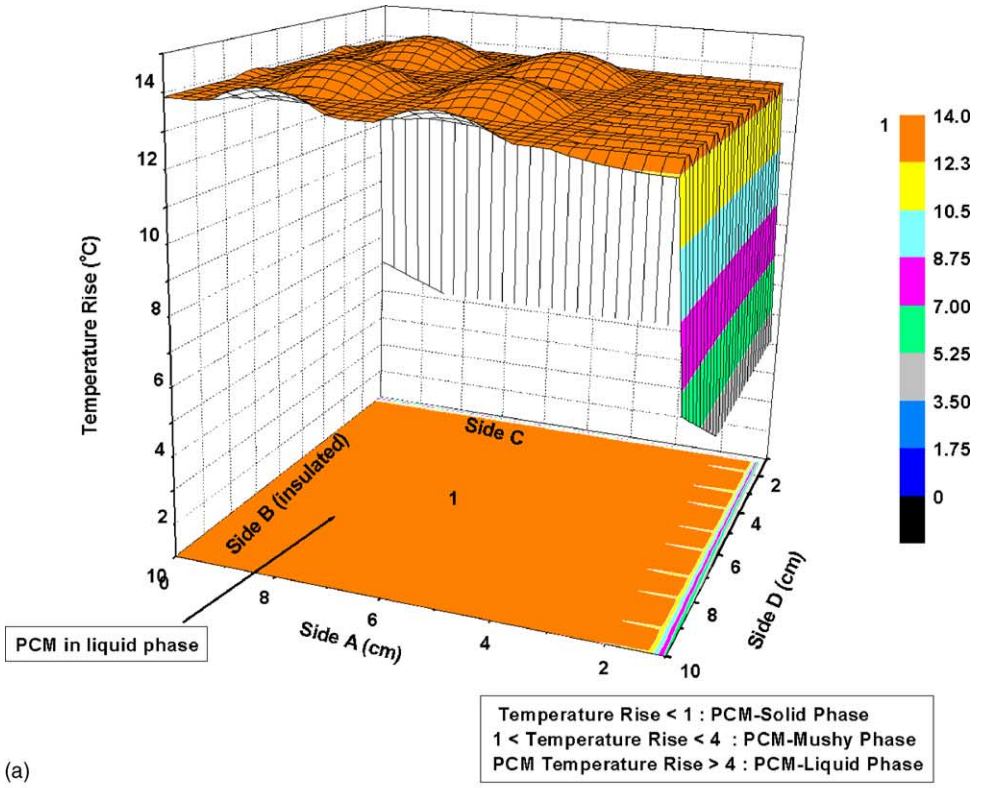

(a)

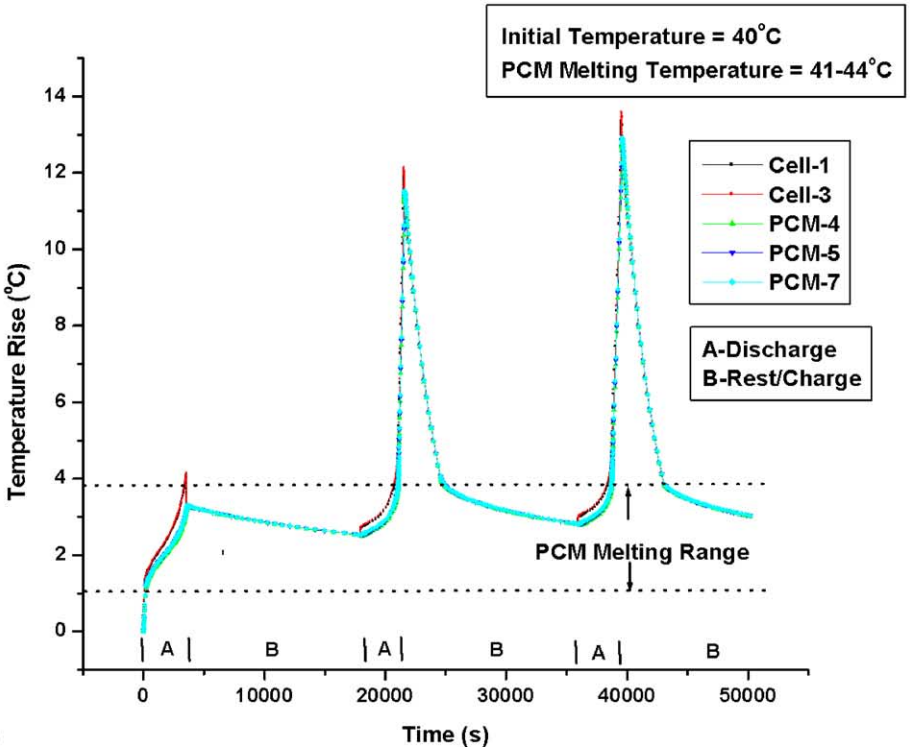

(b)

Fig. 8. (a) Temperature contours of Li-ion cells and PCM during summer. (b) Temperature rise of Li-ion cells and PCM during summer. (c) Effective specific heat of PCM during summer.

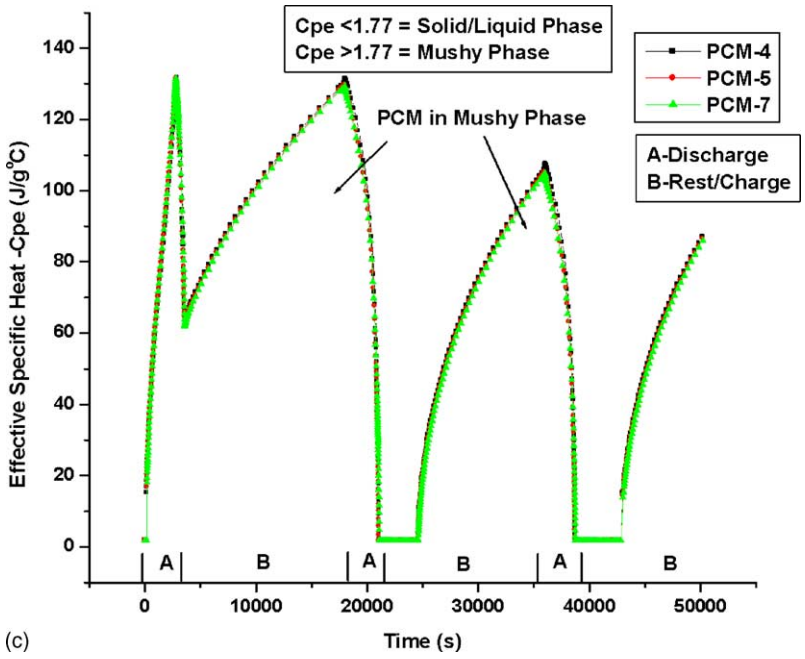

Fig. 8. (*Continued*).

temperature during each cycle. The addition of aluminum fins on the external surface of the module can overcome this problem as explained below.

The temperature contours of the module is shown in Fig. 7(a), depicting the uniform temperature distribution because of the combined effect of the aluminum foam and fins. Fig. 7(b) shows the thermal response of the module with a stable temperature profile of the cells and the PCM as compared to Fig. 6(b). The PCM undergoes complete solidification during the charge/rest period due to the inclusion of aluminum-fins, which boosts the heat dissipation rate from the cells and the PCM when compared to aluminum foam alone. The PCM undergoes little melting during all of the discharge cycles by observing the narrow peaks in Fig. 7(c), indicating that a large latent heat is still available.

From these simulation results, it can be understood that the thermal stability of the entire module requires the addition of aluminum-fins in addition to the aluminum foam. Since our main objective is to replace the existing lead–acid battery with minimal changes in the scooter design, the advantages of the Al-fins can be realized with the presence of the Al-frame covering the battery as shown in Fig. 1, which was not considered in the simulations. Because of its large heat transfer area available, the Al-frame can act as extended heat transfer surfaces for dissipating the heat.

Another important conclusion from this simulation is the availability of the latent heat of the PCM. This can prove to be an effective reserve heat sink in case of a higher ambient temperature or in the event of the battery abuse caused by mechanical crushing or short-circuit, which can result in a thermal runaway situation of the Li-ion cells.

3.5. Case study 4

3.5.1. Performance of the Li-ion battery during the summer and winter conditions

In the previous simulations, the starting temperature of the PCM was assumed to be 30 °C and the temperature rise shown was for this reference temperature. In order to evaluate the adaptability of the PCM to varying climatic conditions, the simulation is performed for the summer and winter ambient temperatures. Since the thermal response of the module is more effective only with the presence of Al-foam and Al-fins, the simulation results are presented for this case alone.

During summer, the reference temperature is chosen to be 40 °C. Hence, as soon as the battery starts discharging, the PCM begins melting and it is very interesting to observe the behavior of the PCM during all the three cycles. The temperature profiles of the Li-ion cells and the PCM region is shown in Fig. 8(a) and (b). In the first discharge cycle, most of the PCM is melted with maximum utilization of the latent heat, resulting in a temperature rise of 4.5 °C. During the following charge/rest period, the PCM does not recover to its original solid phase and stays in the mushy phase at the end of rest period.

The second discharge cycle begins with immediate utilization of the latent heat of the PCM, which regulates the temperature of the Li-ion cells to a minimal increase. But as soon as the PCM turns into a liquid phase, the temperature of the Li-ion cells and the PCM increase significantly as the PCM no more acts a heat sink with the temperature rising by 9 °C. The Li-ion cells and the PCM show similar thermal response during the third discharge cycle with the

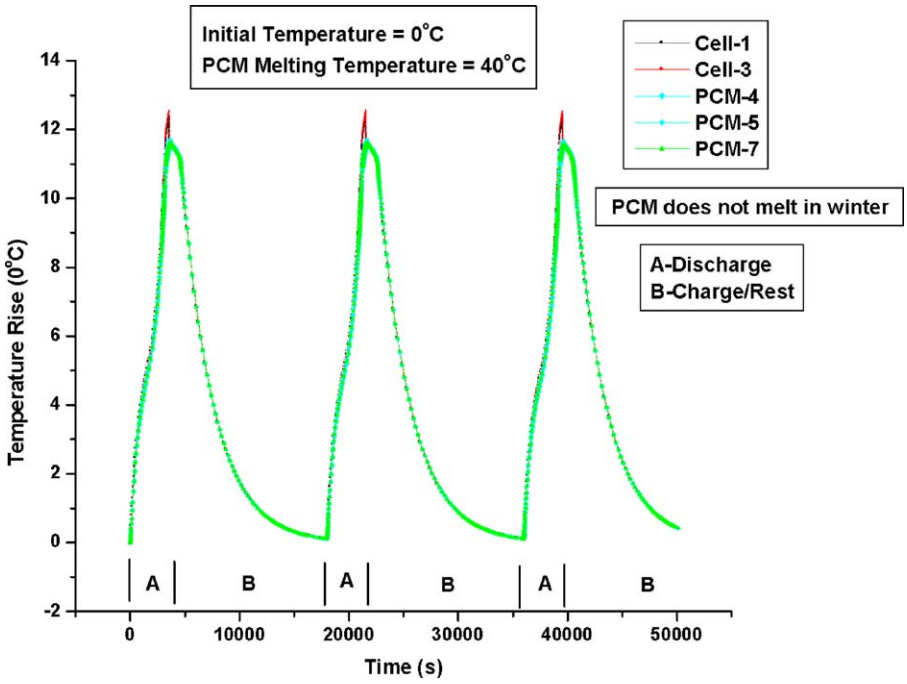

Fig. 9. Temperature rise of Li-ion cells and PCM during winter.

temperature rise of 11 °C at the end of discharge. Hence, the module is expected to be within the safe temperature operating limits in summer which cannot be achieved in the case of an air-cooling system or using PCM alone.

The winter condition was simulated with an initial temperature of 0 °C and the temperature rise is reported with this reference temperature. In this case, only the sensible heat of the PCM is utilized with no melting taking place as seen in Fig. 9. The thermal response of the module is repetitive over all the three cycles.

It should be noted that the electrochemical performance of the Li-ion cells drops at low and elevated temperatures [8]. For simplification purposes, in the above simulations under summer and winter conditions, the temperature effects on the Li-ion cell capacity were neglected and the performance of the Li-ion cell was not altered as compared to the previous simulation.

From the above simulation case studies, the phase change material clearly demonstrates the possibility of achieving an efficient thermal regulation of the Li-ion battery via a simple, inexpensive passive thermal management system.

4. Conclusions

A detailed design procedure of a Li-ion battery containing PCM for thermal management was shown. The thermal response of the Li-ion battery module with air-cooling was evaluated in the presence of Al-fins. The simulation results showed that the Li-ion module was prone to thermal runaway due to inadequate air-cooling. Alternatively, the Li-ion battery can be operated safe only with forced air-cooling, adding to design complexity, addition of many components needed for forced air-cooling and major modifications of the existing scooter.

Simulation results of the Li-ion battery module employing PCM alone indicated that the heat dissipation capability of the PCM is ineffective due to its poor thermal conductivity; furthermore it may cause thermal runaway. The thermal performance of the PCM was significantly improved by the addition of aluminum foam, which increased the thermal conductivity of PCM by one order of magnitude. Though the addition of aluminum foam decreased the temperature rise of the Li-ion battery module by 25 °C, it proved to be ineffective when the electric scooter is driven for continuous three cycles due to the PCM completely melting during the second cycle, risking the battery module to high temperature rise and thermal runaway. Aluminum fins were added to the existing battery module to overcome this problem. Numerous simulations were conducted to obtain a stable temperature profile of the Li-ion battery module by optimizing the length and the number of fins. The aluminum fins proved to be very effective in maintaining the temperature uniformity and suppressing the temperature rise during the three cycles of scooter operation. During the summer operation, the Li-ion battery module showed a temperature rise of 25 °C starting with 40 °C initial temperature, which reflects a safe temperature situation for the Li-ion battery module. There was no melting of the PCM under the winter operating conditions with a start temperature of 0 °C.

In this work, the modeling and the simulation work did not consider the thermal runaway effects during the abuse operating conditions of the Li-ion battery. Future work will incorporate these simulations and also include the experimental

validation of the simulation results presented. The present Li-ion battery design and battery orientation is suggested in order to replace the existing lead–acid battery in the Zappy electric scooter with the Li-ion battery without introducing any mechanical changes in the battery compartment. But an alternative design will feature the aluminum fins on the battery compartment and include modification of the battery compartment to accommodate the Li-ion battery with the PCM system for best heat dissipation effects.

These simulation results prove the feasibility of a well-designed phase change material system as a simple, cost effective thermal management solution for Li-ion batteries in all applications including hybrid electric vehicle.

Acknowledgements

The authors are grateful for the financial support provided by All Cell Technologies, LLC (Chicago, IL) and the ITEC group (Chicago, IL). Technical support by MicroSun Technologies is also acknowledged. The authors thank Andrew Mills for his help in formatting the paper.

References

[1] R.F. Nelson, J. Power Sources 107 (2002) 226–239.
[2] S. Al-Hallaj, H. Maleki, J.S. Hong, J.R. Selman, J. Power Sources 83 (1999) 1–8.
[3] A.A. Pesaran, in: Proceedings of the first Annual Advance Automobile Battery Conference, 5–8 February 2001. http://www.ctts.nrel.gov/BTM.
[4] M. Sung, K.H. Liu, Y.-Y. Wang, C.-C. Wan, J. Power Sources 109 (2002) 160–166.
[5] I. Buchmann, Batteries in Portable World, Chapter 5. http://www.buchmann.ca/toc.asp.
[6] S. Al-Hallaj, J.R. Selman, J. Electrochem. Soc. 147 (9) 3231–3236.
[7] Zappy Technical Manual. http://www.zapworld.com/zappy.htm.
[8] Y. Saito, K. Takano, A. Negishi, J. Power Sources 97–98 (2001) 693–696.
[9] J.R. Selman, S. Al-Hallaj, I. Uchida, Y. Hirano, J. Power Sources 97–98 (2001) 726–732.
[10] J.S. Hong, H. Maleki, S. Al-Hallaj, L. Redey, J.R. Selman, J. Electrochem. Soc. 145 (5) 1489–1501.
[11] S. Al-Hallaj, J. Prakash, J.R. Selman, J. Power Sources 87 (2000) 186–194.
[12] J.P. Holman, Heat Transfer, 7th Ed., McGraw Hill, New Jersey, 1992.
[13] A.M. Andersson, K. Edström, J.O. Thomas, J. Power Sources 81–82 (1999) 8–12.
[14] P. Nelson, D. Dees, K. Amine, G. Henriksen, J. Power Sources 110 (2002) 349–356.
[15] http://www.cpsc.gov/cpscpub/prerel/prhtml02/02251.html; http://www.EVGlobal.com.
[16] K. Kelly, M. Zolot, M. Mihalic, Battery usage and thermal performance of the Toyota Prius and Honda insight for various chassis dynamometer test procedures, in: Proceedings of the 17th Annual Battery Conference on Applications and Advances, Long Beach, CA, January 2002.
[17] M.M. Farid, F.A. Hamad, M.A. Arabi, Energy Conv. Manage. 39 (8) (1998) 809–818.
[18] ERG Materials and Aerospace Corporation, 900 Stanford Avenue, Oakland, CA, Technical manual. http://www.ergaerospace.com/.
[19] A. Sullins, K. Daryabeigi American Institute of Aeronautics and Astronautics, in: Proceedings of the 35th AIAA Thermophysics Conference, AIAA 2001–2819.
[20] R.B. Wright, C.G. Motloch, J.R. Belt, J.P. Christophersen, C.D. Ho, R.A. Richardson, I. Bloom, S.A. Jones, V.S. Battaglia, G.L. Henriksen, T. Unkelhaeuser, D. Ingersoll, H.L. Case, S.A. Rogers, R.A. Sutula, J. Power Sources 110 (2002) 445–470.